Journal of Power Sources 240 (2013) 612–617

Contents lists available at SciVerse ScienceDirect

Journal of Power Sources

journal homepage: www.elsevier.com/locate/jpowsour

Miniature H_2/O_2 fuel cells using TiO_2 nanotube substrates and sputtered Pt catalyst

Woo-Jin Lee, Dong-Ha Lim, W.H. Smyrl*

Corrosion Research Center, Department of Chemical Engineering and Materials Science, University of Minnesota, 421 Washington Ave SE, Minneapolis, MN 55455, USA

HIGHLIGHTS

- Novel Ti substrates support Pt/titanium dioxide nanotubes (TONT) catalysts.
- Pt sputtered on porous Ti/TONT support the oxygen reduction reaction at low loading.
- Pt/Ti(microgrid)/TONT electrodes deliver excellent power in H2/O_2 fuel cells.

ARTICLE INFO

Article history:
Received 8 February 2013
Received in revised form
11 April 2013
Accepted 7 May 2013
Available online 16 May 2013

Keywords:
Miniature fuel cell
Titanium oxide nanotube
Electrochemical anodization methods
Oxygen reduction reaction

ABSTRACT

Modified designs for a miniature H_2/air fuel cell are described using Pt sputtered on titanium oxide nanotube (Pt/TONT) as a catalyst at low mass loadings. Titanium microgrids or Ti evaporated onto a silicon substrate with holes at the center were used as substrates that were then anodized in fluoride-containing electrolytes to form the TONT arrays. Self-organized tubes grew as anodizing time increased, resulting in the highly enhanced surface area for electrochemical reactions. High cathodic current on cyclic voltammogram of Pt/TONT catalyst indicated high catalytic activity for the oxygen reduction reaction (ORR). The miniature fuel cells were successful, and showed high power densities up to 9.64 mW cm^{-2} at potentials from 0.7 V to 0.2 V.

1. Introduction

Miniature fuel cells have emerged recently as good power sources for micro-aerial vehicles (MAVs), robots and many small power computer, communication, and consumer electronics [1]. The rapid development of miniature cells has been driven by increased demands for miniature power sources. In order for miniature fuel cells to be viable for small power applications, several problems such as cell design, low reliability, poor performance and durability must be solved. Many research groups have recently given attention to the development of miniature or micro fuel cells by various methods such as microelectromechanical systems (MEMS) technology and alternative cell designs that use air instead of pure O_2 gas [1–10]. A high performance electrode for the miniature polymer electrolyte fuel cell (PEFC) used in the previous research at the University of Minnesota was produced on silicon (Si) substrates using traditional Si micro-fabrication procedures adapted from the MEMS and electronics industries [11a,b].

A major objective is to lower the amount of catalyst needed for efficient performance and to facilitate design of membrane electrode assemblies (MEAs) that have effective catalyst distributions. There is recent research in forming and utilizing ordered TiO_2 nanotube (TONT) arrays as electrode materials for fuel cell applications [12–16]. Recently, we have reported on the synthesis and characterization of Pt sputtered onto the TONT array structures with excellent electrochemical properties and durability for polymer electrolyte fuel cells [13–15].

Sputter deposition is a clean, fast, reliable, flexible method to form catalytic structures on chosen substrates. Single metals and alloys deposited by single-gun or multiple-gun sources provide excellent materials for evaluation of catalyst/substrate combinations [13–15]. In our research, we found that the sputtered Pt/TONT catalyst with low mass loadings of Pt has promise as a cathode for the oxygen reduction reaction (ORR) in fuel cell applications. To enhance the performance, this paper reports on developing two

* Corresponding author. Tel.: +1 612 625 0717; fax: +1 612 626 7246.
E-mail address: smyrl@umn.edu (W.H. Smyrl).

0378-7753/$ – see front matter © 2013 Published by Elsevier B.V.
http://dx.doi.org/10.1016/j.jpowsour.2013.05.029

substrates and designs of miniature FCs using Pt/TONT catalysts on porous substrates to enhance the surface area and to improve cell behavior. The two substrates used here are: (1) Ti microgrid electrodes, and; (2) sputtered Ti thin films on microfabricated Si wafers.

2. Experimental

2.1. Fabrication of Ti microgrid electrodes

The titanium microgrid substrates (DEXMET, Naugatuck, CT) had Ti ribs of 76 μm, and diamond-shaped openings of 1956 μm. A strip was cut from the commercial sheet, and partially immersed in a solution of 0.5 wt% HF(aqueous). A voltage of +20 V was applied for 20 min between this electrode and a Pt counter electrode to form TiO_2 nanotubes (TONT) as we introduced earlier [9]. The microgrid electrode was removed from solution, rinsed with high purity DI water, and soaked in DI water for at least 5 min. The TONT/microgrid was dried in a pure N_2 gas stream. Samples were heat treated in air for 3 h at 300 °C to convert the TONT array to crystalline anatase, and to remove residual fluorine species [12–15].

2.2. Fabrication of mini-FC electrodes on Si wafers

The mini-FC electrodes on silicon wafer substrates were prepared using a series of fabrication steps as previously reported [11a,11b]. Individual mini-FC chips with the size of 2.5 cm × 2.5 cm were separated by cleavage of the finished wafers. In a final photolithography step, a total of 5184 gas feed-holes (25 μm × 25 μm) were patterned and etched over a 0.5 cm × 0.5 cm area, using a deep-trench reactive ion etcher, through both the gold electrodes and the Si membranes [11b]. Using E-beam evaporation (SCE-600, CHA Industries) under a vacuum of 5×10^{-5} mbar with a graphite crucible, we first evaporated 750 nm thick Ti film on the gold-coated Si membrane located at the center of the FC chip, where the gas feed-holes had been formed. For TONT formation, Ti-evaporated FC chips were anodized in an aqueous solution of 1 M Na_2SO_4 + 0.2 M citric acid + 0.5 wt.% NaF at +10 V for various anodizing times (150, 300, and 600 s), using a Pt counter electrode. After that, the TONT FC chips were heat treated at 300 °C for 3 h in ambient air. The above modified solution and procedure was successful, and the fabrication success rate approached 100%. We note that using aqueous HF solutions on the sputtered Ti films caused lift-off of the gold-field beneath the Ti film on the Si substrate, so the alternate electrolyte was developed to limit the attack and lift-off from the Si substrates.

2.3. Preparation of Pt/TONT catalyst on Ti microgrid electrodes and on mini-FC Si wafer substrates

The catalyst for the Ti microgrid and mini-FC chips were thin Pt (10 or 20 nm; 21 or 42 μg cm^{-2}, respectively) layers deposited on the TONT region by sputtering at 250 W dc power, a pressure of 2 Pa, and room temperature (AJA Sputter System) [13]. The sputter system is calibrated to deliver deposits of selected film thickness on planar substrates, assuming uniform deposition. To address the structural and morphological characterization of Pt/TONT catalysts, a JEOL 6500 field emission scanning electron microscopy (FE-SEM, JEOL Inc.) operating at 5 kV and 10 mA was used. We note that the microgrid substrates had 72% open area between Ti strands. Thus, much of the sputtered Pt did not deposit on the Ti strands, but instead passed through to deposit onto the metal foil underneath. We assume here that the mass of sputtered Pt on the Ti microgrids had the same mass loading per area as for a planar substrate after correcting for the lower area available for deposition.

2.4. Assembly of fuel cells with microgrid Pt/TONT electrodes

The procedure previously reported for Flex-FCs [13] was adapted for the microgrid samples. A central Nafion 117 membrane was sandwiched on either side with a microgrid Pt/TONT electrode. To improve contact between Nafion with the electrodes, each of the electrodes was treated first with 5 μL of Nafion solution (5 wt%, Sigma Aldrich) that was spread over the active region of the microgrid electrodes. This procedure deposited 1.28 mg cm^{-2} of Nafion on the microgrid electrode (corrected for surface area of Ti microgrid). The Nafion deposit was allowed to dry for a few minutes, and then each electrode was placed on the central Nafion membrane for assembly into the final cell with our lamination procedure [13]. An assembled microgrid fuel cell was clamped mechanically onto a glass manifold gas delivery system for testing. Current *vs.* voltage (*I*–*V*) measurements utilized a potentiostat (Solatron 1287) while the gases were supplied from pressurized, high purity H_2 and air tanks. The gases were humidified before delivery (150 ml min^{-1}) to the anode and cathode electrodes, respectively. Experiments were carried out under ambient conditions (~25 °C and ambient pressure).

2.5. Si wafer Mini-FC assembly and testing

The Si wafer mini-FC electrodes were hot-pressed onto either side of a Nafion 117 membrane, with the active area of Pt/TONT on the gas feed-hole substrate. Then, wire leads were soldered onto the gold contact pads as current collectors. The construction of a Si wafer mini-FC is shown in Fig. 1. An assembled mini-FC was clamped mechanically onto a glass manifold gas delivery system for testing as reported previously [15,17]. Current *vs.* voltage (*I*–*V*) measurements utilized a potentiostat (Solatron 1287) while the gases were supplied from pressurized, high purity H_2 and air tanks. The gases were humidified before delivery (150 ml min^{-1}) to the anode and cathode electrodes, respectively. All experiments were carried out under ambient condition (~25 °C and ambient pressure).

2.6. Electrochemical measurements for ORR activity

Before cell assembly, each Si wafer mini-FC electrode with Pt/TONT catalyst was electrochemically evaluated by cyclic voltammetry (CV) using a Solatron 1287 Electrochemical Interface under software control at room temperature in either He-purged or O_2-saturated 0.5 M $HClO_4$ solution. Electrochemical experiments were conducted in a three-electrode cell with Pt/TONT catalyst as the working electrode, a saturated calomel electrode (SCE) as the reference electrode, and a platinum wire as the counter electrode. For all CV experiments, the potential was scanned at 2 mV s^{-1} from 0.1 to 0.9 V (vs. SCE).

3. Results and discussion

3.1. Pt/TONT catalyst on Ti microgrid substrates

Fig. 2 shows the SEM micrographs of the TONT arrays formed on the Ti microgrid. It was found previously [13] that nanotubes were always perpendicular to the Ti substrate for planar, circular rods, wires,and screw geometries. The TONT arrays here are perpendicular to all the surfaces of the microgrid substrates as well. After Pt was sputtered onto one side of the microgrid sheet (mass loading of 42 μg cm^{-2}), the substrate was flipped over, and Pt was sputtered onto the other side as well (same amount of Pt on each side, total of 84 μg cm^{-2}). With Pt on both sides, the total current was found to be nearly twice that for one-side Pt only. If the bare TONT (with no Pt on one side) was arranged to face the Nafion membrane, and the

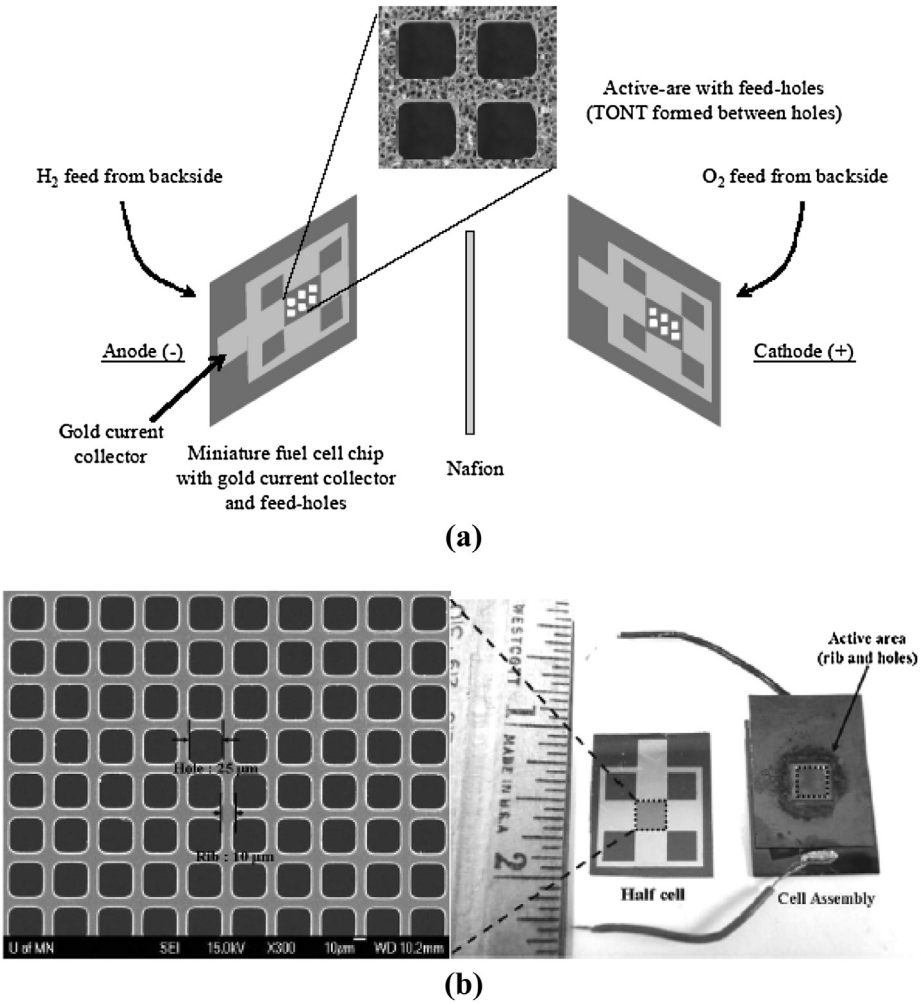

Fig. 1. (a) Exploded view of mini-FC assembly. Illustration shows placement of chips with Pt/TONT catalyst, and Nafion membrane. Hot-pressing laminates these layers together in a "sandwich" construction. (b) Photos of center region with holes and rib (left) and mini-FC assembly (right).

sputtered side (Pt/TONT) faced away, there was substantial current. If the bare side faced out and the catalyzed side faced the Nafion membrane, the current was higher but lower than that where both sides were catalyzed. We conclude that TONT formed on the sidewalls of the microgrid had some sputtered Pt on this region of the array, but the Pt mass coverage on the sidewalls was probably smaller than on either side of the microgrid facing outward. We note also that addition of the Nafion solution added to the TONT/microgrid also facilitated electrochemical reactions on the sides and back of the microgrid sheet. We found that 5 μL of Nafion solution was optimum for our conditions, and that 10 μL did not increase the total current substantially. In Fig. 2, the added Nafion (5 μL) is not apparent in the SEM, but when 10 μL was added a web of polymer was seen at the junctions of the Ti ribs.

3.2. Formation of Pt/TONT catalyst on Si wafer mini-FC electrodes

Fig. 3 shows the SEM micrographs of the Ti film evaporated onto the FC chip samples, anodized in 1 M Na_2SO_4 + 0.2 M citric acid + 0.5 wt.% NaF solution under +10 V constant voltage for different anodizing times. The formation sequence of TONT arrays can be clearly understood from the figures. In the initial stage of formation, the original evaporated Ti film morphology (as seen in Fig. 3a) is mostly transformed to a porous structure by 150 s (Fig. 3b). As the anodization progresses, the top view shows regular morphology with 40–60 nm sized platelets, which become the bottoms of the TONT vertically grown from them by 300 s (Fig. 3c).

After the anodization time of 600 s, as shown in images at high magnification (see in the inset of Fig. 3d), TONT with ca. 40–60 nm diameter and ca. 30–50 nm hole size are uniformly distributed perpendicular to the surfaces of mini-FC chip in a regular pattern. The nanotubes were smaller in dimension with a periodic ring structure as compared to results reported elsewhere [12,18,19]. We find that this robust direct fabrication of TiO_2 nanostructure with well-aligned morphology, orientation, and surface architectures was successfully formed on the patterned Si wafer FC chip.

After optimizing an anodization time to make a TONT on the mini-FC chip, the 10 or 20 nm thick Pt layer was deposited on the TONT surface by sputtering. Fig. 4 depicts the SEM views of 10 and 20 nm thick Pt sputtered on TONT arrays formed on mini-FC chips. We can see that nanometer sized Pt deposits were formed on the upper rim of TONT arrays, depending on the sputtering thickness. The Pt sputtered particles were rigidly attached on the rims with a high fidelity to the original TONT surface morphology, preserving an enhanced surface area.

3.3. Catalytic activity for the oxygen reduction reaction (ORR)

Fig. 5 shows ORR curves for the 10 and 20 nm thick Pt sputtered on TONT on Si wafer FC chips measured at a scan rate of 2 mV s^{-1} in

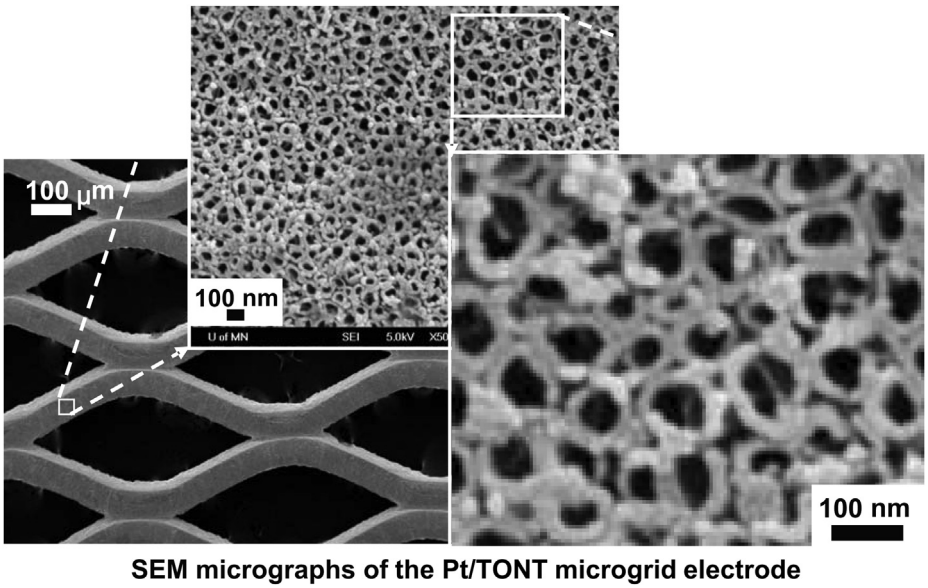

Fig. 2. SEM micrographs of Pt/TONT microgrid electrodes with 20 nm sputtered Pt on each side and 5 nL of Nafion solution spread over the TONT active area.

O_2-saturated 0.5 M $HClO_4$ electrolyte solution at room temperature. The ORR curves were cycled from 0.9 V to cathodic direction down to 0.1 V (vs. SCE). As shown in Fig. 5, ORR curves for both Pt loadings are controlled by diffusion (below 0.2 V), mixed diffusion kinetics (0.2–0.6 V), and kinetics (above 0.6 V) in the different potential regions. All the CV data show cathodic limiting current fluctuations at lower potentials around 0.2 V, where the reduction reaction is mass transfer controlled [13]. It is noted that the reduction current is enhanced in O_2-saturated electrolyte solution as compared to that in He-purged electrolyte solution. This indicates the viable activity of Pt/TONT catalyst for O_2 reduction. In addition, there was a positive shift of ~72 mV of the onset potential and ~56 mV in the half-wave potential of 20 nm thick Pt sputtered on TONT in compared with those of 10 nm thick Pt sputtered on TONT. Furthermore, the ORR current increases with increasing the Pt thickness from 10 to 20 nm, representing an increase in catalytic

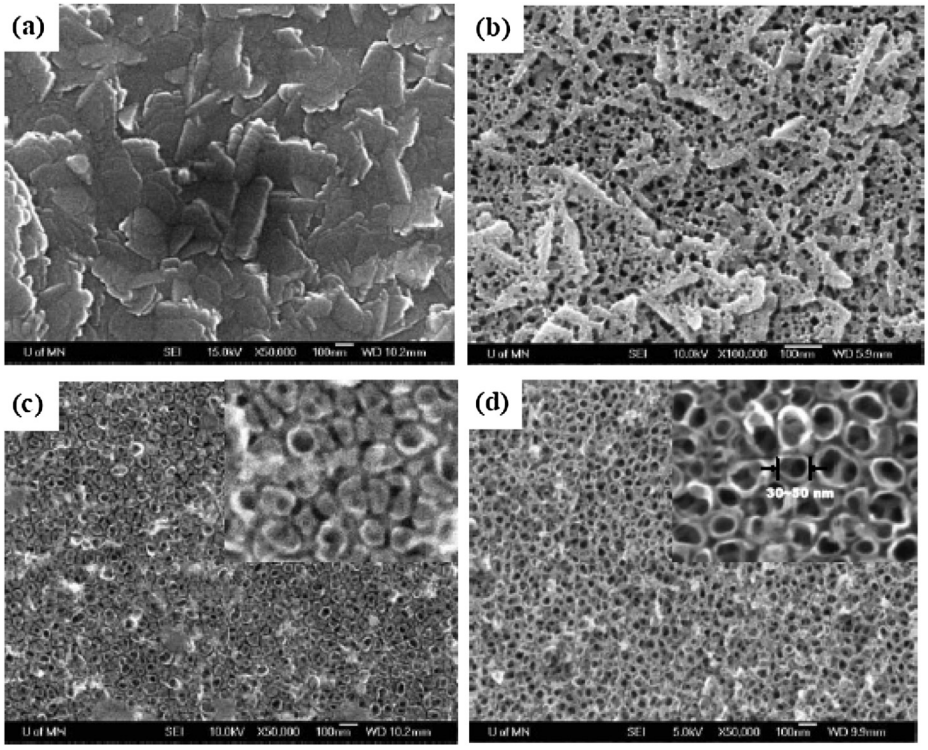

Fig. 3. SEM micrographs of TONT formed on Si substrate by anodizing in 1 M Na_2SO_4 + 0.2 M citric acid + 0.5 wt.% NaF solution at 10 V for anodization times of (a) 0 s (750 nm evaporated Ti surface), (b) 150 s, (c) 300 s, and (d) 600 s.

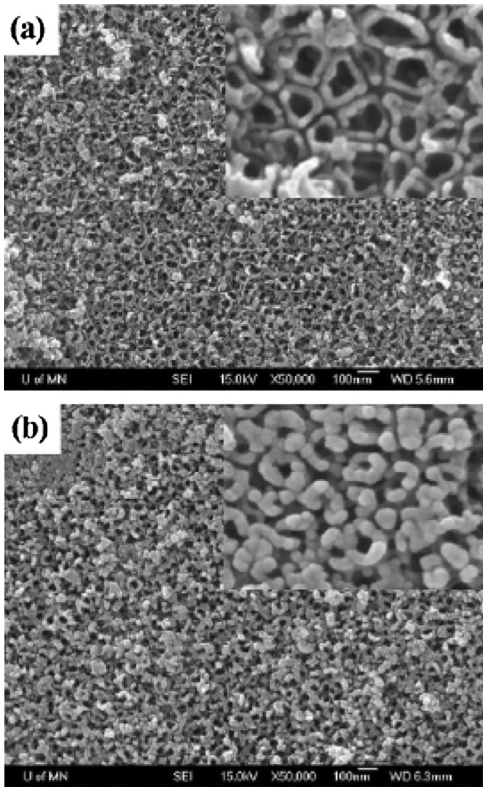

Fig. 4. SEM micrographs of (a) 10 nm and (b) 20 nm thick Pt/TONT catalyst formed on mini-FC chips.

activity. This is attributed to enhanced conductivity down along the inside of the nanotubes with increasing Pt loading on the surface [20].

3.4a. Performance of Pt/TONT/Ti microgrid FC

The *I–V* characteristics and the power density for Ti microgrid FC performance were measured at room temperature. The power density reached a maximum of 2.7 mW at 0.45 V. This compares favorably to our previous studies [13]. When the single cell was held at 0.5 V for 24 h, the power decreased from 2.7 to 2.4 mW (~11.3% decrease). We cannot explain the small decrease at this time, but further work will focus on increasing the overall performance and eliminating the temporal decrease.

3.5. Performance of Si wafer mini-FC testing

Fig. 6 shows *I–V* characteristics together with power density variation, obtained from the mini-FC test at room temperature. The mini-FC runs successfully with H_2/air at potentials ranging from 0.7 to 0.2 V. In the case of 10 nm thick Pt sputtered on TONT, the maximum power density reached 3.3 mW cm^{-2}, corresponding to the current density of 12.5 mA cm^{-2} at 0.25 V. For a 20 nm thick-sputtered Pt layer, the maximum power density was improved to 4.6 mW cm^{-2} at a current density as high as 16.4 mA cm^{-2} and a voltage of 0.28. There is about 39% power increase with increased Pt loading. These values need to be improved to match the best value of 11.2 mW cm^{-2} at 40 mA cm^{-2} and 0.28 V, obtained from our previous mini-FC using 2.5 mg cm^{-2} unsupported Pt black on cathode and 4.0 mg cm^{-2} Pt/Ru electrodeposited on anode [11].

The Si wafer mini-FCs had higher apparent current densities and higher power densities as compared to the Ti microgrid FCs.

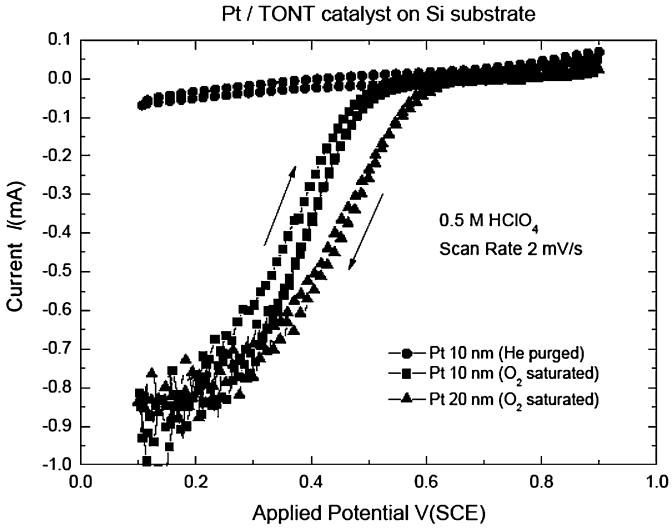

Fig. 5. Cyclic voltammograms of the Pt/TONT catalyst in 0.5 M $HClO_4$ electrolyte solution at conditions of (●) 10 nm Pt/TONT with He purge, (■) 10 nm Pt/TONT with O_2 saturation, and (▲) 20 nm Pt/TONT with O_2 saturation.

However, the results for microgrid FCs are for surface areas considerably smaller than for the mini-FCs. The apparent area (i.e. projected area) of the Si wafer mini-FC electrodes was estimated to be 0.117 cm^2. Because the open area between the Ti strands in the microgrid substrates was relatively large, the effective catalytic area was smaller. We estimate that the Ti microgrid area is about 28% of the total projected area of Ti strands plus 72% for the open region between strands. The current density and power density of the microgrid samples could be corrected by multiplying by 1/28 = 3.57. That is, the maximum power density for the microgrid FCs would be 3.57 × 2.7 mW = 9.64 mW cm^{-2} (corrected), i.e. larger than the mini-FCs but smaller than 11.2 mW cm^{-2} reported in our earlier work.

Further, we can see that the current density values obtained from the Si wafer mini-FC are lower than those values for O_2 reduction on the Pt/TONT surface immersed in 0.5 M $HClO_4$ electrolyte solution as shown in cyclic voltammograms (Fig. 5). The Si wafer mini-FC needs design improvement to increase the current. Of primary importance perhaps is limited access of the reactant gases to the Pt/TONT areas located between the gas feed-holes on

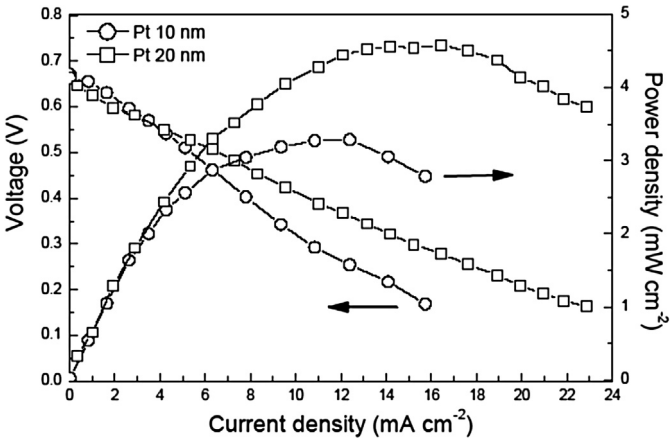

Fig. 6. *I–V* characteristics and power density of mini-FC using (○) 10 nm and (□) 20 nm thick Pt/TONT catalyst [conditions: ambient pressure, RT, H_2 and air gases (150 ml min^{-1})].

the Si wafer chips. The results represent progress in utilizing the Pt/TONT catalyst on both substrate supports. The catalyst/support systems are a cheap and more durable alternative to carbon substrates [21].

4. Conclusions

The present designs using the robust TiO_2 nanotube (TONT) supports formed by electrochemical anodization, successfully miniaturizes H_2/air gas-feeding fuel cell. Using 20 nm thick Pt/TONT catalyst, the maximum power density for Ti microgrid FCs reached 2.7 mW cm^{-2}. When corrected for area, the Ti microgrid FCs reached 9.64 mW cm^{-2}. The mini-FC cell was found to have 4.6 mW cm^{-2} at current densities of 16.4 mA cm^{-2}. On the basis of the experimental findings, we have demonstrated the promising application of TiO_2 nanotube structures to catalyst materials as an alternative for fuel cells using direct tailoring of their morphology. We recently found that the Pt/TONT catalysts were much more durable than Pt C catalysts [21].

Acknowledgments

This research was supported by the Initiative for Renewable Energy and the Environment of the University of Minnesota, project no. LG-MC3-2005 and by the collaborative project funded by King Abdulaziz City for Science and Technology, Riyadh, Saudi Arabia.

References

[1] C.-Y. Chen, W.-H. Lai, B.-J. Weng, H.-J. Chuang, C.-Y. Hsieh, C.-C. Kung, J. Power Sources 179 (2008) 147.
[2] R. Hahn, S. Wagner, A. Schmitz, H. Reichl, J. Power Sources 131 (2004) 73.
[3] K. Shah, W.C. Shin, R.S. Besser, Sens. Actuators B 97 (2004) 157.
[4] B.Y. Park, M.J. Madou, J. Power Sources 162 (2006) 369.
[5] P.-C. Lin, B.Y. Park, M.J. Madou, J. Power Sources 176 (2008) 207.
[6] S. Tominaka, S. Ohta, H. Obata, T. Momma, T. Osaka, J. Am. Chem. Soc. 130 (2008) 10456.
[7] J. Yu, P. Cheng, Z. Ma, B. Yi, Electrochim. Acta 48 (2003) 1537.
[8] N. Wan, C. Wang, Z. Mao, Electrochem. Commun. 9 (2007) 511.
[9] Y. Zhang, J. Lu, S. Shimano, H. Zhou, R. Maeda, Electrochem. Commun. 9 (2007) 1365.
[10] Y. Lu, R.G. Reddy, Electrochim. Acta 54 (2009) 3952.
[11] (a) S.C. Kelley, G.A. Deluga, W.H. Smyrl, Electrochem. Solid-state Lett. 3 (2000) B407;
(b) S.C. Kelley, G.A. Deluga, W.H. Smyrl, AIChE J. 48 (5) (2002) 1071.
[12] W.-J. Lee, M. Alhosan, W.H. Smyrl, J. Electrochem. Soc. 153 (2006) B499.
[13] W.-J. Lee, M. Alhosan, S.L. Yohe, N.L. Macy, W.H. Smyrl, J. Electrochem. Soc. 155 (2008) B915.
[14] S.-H. Kang, Y.-S. Sung, W.H. Smyrl, J. Electrochem. Soc. 155 (2008) B1128.
[15] D.-H. Lim, W.-J. Lee, N.L. Macy, W.H. Smyrl, Electrochem. Solid-state Lett. 12 (2009) B123.
[16] Y. Fu, Z.D. Wei, S.G. Chen, L. Li, Y.C. Feng, Y.Q. Wang, X.L. Ma, M.J. Liao, P.K. Shen, S.P. Jiang, J. Power Sources 189 (2009) 982.
[17] J. Wheldon, W.-J. Lee, D.-H. Lim, A.B. Broste, M. Bollinger, W.H. Smyrl, Electrochem. Solid-state Lett. 12 (2009) B86.
[18] D. Gong, C.A. Grimes, O.K. Varghese, W. Hu, R.S. Singh, Z. Chen, E.C. Dickey, J. Mater. Res. 16 (2001) 3331.
[19] R. Beranek, H. Hildebrand, P. Schmuki, Electrochem. Solid-state Lett. 6 (2003) B12.
[20] L. Yang, D. He, Q. Cai, C.A. Grimes, J. Phys. Chem. C 111 (2007) 8214.
[21] D.-H. Lim, W.-J. Lee, J. Wheldon, N.L. Macy, W.H. Smyrl, J. Electrochem. Soc. 157 (6) (2010) B862–B867.